

# Multi-Spatial Scale Dynamic Interactions between Functional Sources Reveal Sex-Specific Changes in Schizophrenia

A. Iraj<sup>1,\*</sup>, A. Faghiri<sup>1</sup>, Z. Fu<sup>1</sup>, S. Rachakonda<sup>1</sup>, P. Kochunov<sup>2</sup>, A. Belger<sup>3</sup>, J.M. Ford<sup>4,5</sup>, S. McEwen<sup>6</sup>, D.H. Mathalon<sup>4,5</sup>, B.A. Mueller<sup>7</sup>, G.D. Pearlson<sup>8</sup>, S.G. Potkin<sup>9</sup>, A. Preda<sup>9</sup>, J.A. Turner<sup>10</sup>, T.G.M. van Erp<sup>11</sup>, and V.D. Calhoun<sup>1,\*</sup>

<sup>1</sup>Tri-Institutional Center for Translational Research in Neuroimaging and Data Science (TReNDS), Georgia State University, Georgia Institute of Technology, and Emory University, Atlanta, GA, USA

<sup>2</sup>Maryland Psychiatric Research Center, Department of Psychiatry, School of Medicine, University of Maryland, Baltimore, MD, USA

<sup>3</sup>Department of Psychiatry, University of North Carolina, Chapel Hill, NC, USA

<sup>4</sup>Department of Psychiatry, University of California San Francisco, San Francisco, CA, USA

<sup>5</sup>San Francisco VA Medical Center, San Francisco, CA, USA

<sup>6</sup>Department of Psychiatry and Biobehavioral Sciences, University of California Los Angeles, Los Angeles, CA, USA

<sup>7</sup>Department of Psychiatry, University of Minnesota, Minneapolis, MN, USA

<sup>8</sup>Departments of Psychiatry and Neuroscience, Yale University, School of Medicine, New Haven, CT, USA

<sup>9</sup>Department of Psychiatry and Human Behavior, University of California Irvine, Irvine, CA, USA

<sup>10</sup>Department of Psychology, Georgia State University, Atlanta, GA, USA

<sup>11</sup>Clinical Translational Neuroscience Laboratory, Department of Psychiatry and Human Behavior, University of California Irvine, Irvine, CA, USA

\* Correspondence address to:

armin.iraji@gmail.com (Armin Iraj)

vcalhoun@gsu.edu (Vince Calhoun)

## Abstract

We introduce an extension of independent component analysis (ICA), called multiscale ICA (msICA), and design an approach to capture dynamic functional source interactions within and between multiple spatial scales. msICA estimates functional sources at multiple spatial scales without imposing direct constraints on the size of functional sources, overcomes the limitation of using fixed anatomical locations, and eliminates the need for model-order selection in ICA analysis. We leveraged this approach to study sex-specific and -common connectivity patterns in schizophrenia.

Results show dynamic reconfiguration and interaction within and between multi-spatial scales. Sex-specific differences occur (1) within the subcortical domain, (2) between the somatomotor and cerebellum domains, and (3) between the temporal domain and several others, including the subcortical, visual, and default mode domains. Most of the sex-specific differences belong to between-spatial scale functional interactions and are associated with a dynamic state with strong functional interactions between the visual, somatomotor, and temporal domains and their anticorrelation patterns with the rest of the brain. We observed significant correlations between multi-spatial-scale functional interactions and symptom scores, highlighting the importance of multiscale analyses to identify potential biomarkers for schizophrenia. As such, we recommend such analyses as an important option for future functional connectivity studies.

## Keywords

multi-spatial scale dynamic functional connectivity, multi-spatial scale intrinsic connectivity networks, multi-model-order independent component analysis (ICA), multiscale ICA (msICA), resting-state fMRI

## 1. INTRODUCTION

### 1.1. Multi-Spatial Scale Dynamic Interactions

Brain function has been modeled as coordination and interactions between functional sources, which has been summarized via the principles of segregation and integration (Genon *et al.*, 2018). In other words, the brain can be segregated into distinct functional sources (e.g., intrinsic connectivity networks, ICNs), which dynamically interact with each other (i.e., functional integration). Notably, functional sources exist at different spatial scales, and dynamic functional interactions occur both within and between different spatial scales. However, most approaches typically use a single atlas or network parcellation, rather than attempting to capture dynamics occurring at multiple spatial scales (e.g., evaluating different levels of spatial clustering).

Furthermore, most functional connectivity studies do not consider that a region can simultaneously contribute to several temporally coherent sources at one or multiple spatial scales. There are two general categories of functional connectivity approaches. The first category uses fixed anatomical locations/segmentation (e.g., a sphere with the same radius or predefined structural/functional atlases) as a primitive representation of functional sources. However, studying brain function requires a proper estimation of functional sources (i.e. to ensure voxels groups within the selected ROIs are indeed strongly

temporally coherent with themselves and less temporally coherent with other ROIs) to prevent incorrect functional connectivity inferences (Iraji *et al.*, 2020b). Furthermore, this category almost always assigns each brain region to only one functional source and overlooks the possibility that a region can contribute to several functional sources in one or multiple spatial scales (for example, one can jointly evaluate the degree to which the posterior cingulate (PC) contributes to the default mode network (DMN) as a whole and the degree to the PC contributes to the left parietal subnode of the DMN). Using a fixed seed or region also disregards inter-subject differences of functional sources. The second category utilizes data-driven approaches like independent component analysis (ICA) to identify functional sources and calculates the functional connectivity between them. While this category of studies focuses on estimating subject-specific functional sources, their results are also predetermined by the spatial scale of interest (e.g., model order choice in ICA analysis). Consequently, most studies capture within single-scale functional connectivity, overlooking the functional interactions between functional sources at multiple spatial scales. In a nutshell, while previous works highlight the importance of multiscale analysis (Li *et al.*, 2018), most functional connectivity research focuses on one spatial scale. There is no work to study static and dynamic interactions between functional sources, both within and between multiple spatial scales. Therefore, it is important to develop multi-spatial scale dynamic approaches to study brain function and its changes across various mental states and disorders.

Here, we present an approach that combines multiscale ICA (msICA) and dynamic functional network connectivity (dFNC) to study dynamic multi-spatial scale functional interactions. msICA uses multi-model-order ICA to estimate functional sources at multiple spatial scales. Because of that, it does not impose a direct constraint on the spatial extent of functional sources and does not force the functional sources of a given spatial scale to have the same spatial size. msICA lets the data decides the spatial distribution of functional sources, which gives msICA a great advantage as we do not expect different brain areas, for example, the primary cortex vs the frontal lobe to be parceled at the same rate. Multiscale ICA also addresses the model-order selection problem as, in general, one remedy to parameter selections is finding a procedure to combine results from several parameters. We leveraged this approach to study sex-specific and sex-common schizophrenia differences, which have been understudied but may play an important role in understanding the neural mechanisms as it is clear there are sex differences in schizophrenia, for example in disease onset (Nawka *et al.*, 2013; Li *et al.*, 2016).

## 1.2. Intrinsic Connectivity Networks (ICNs): Assessment of Functional Sources

A functional source can be defined as a temporally synchronized pattern (Iraji *et al.*, 2020b), and studying brain function requires a proper estimation of functional sources to prevent incorrect functional connectivity inferences (Iraji *et al.*, 2020b). Due to its emphasis on capturing sources that are spatially distinct and temporally coherent, ICA has proven itself as a strong method to identify functional sources at different spatial scales from spatially focal, highly granular functional units (Iraji *et al.*, 2019b) to distributed, large-scale brain networks (Iraji *et al.*, 2016). ICA is a data-driven multivariate technique that has been widely applied to functional magnetic resonance imaging (fMRI) data and divides the brain into overlapping functionally distinct patterns, called intrinsic connectivity networks (ICNs). Each ICN is a temporally synchronized pattern of the brain, a good estimation of a functional source. The ICN time course describes its functional activity over time, while its spatial pattern indicates the contribution of spatial locations to ICN. The spatial scale of ICNs can be set effectively using the model orders of ICA. In other words, we can study brain segregation at different spatial scales by using ICA with different model orders. Low-model order ICAs result in large-scale spatially distributed ICNs while higher model order results in more spatially granular ICNs. While there have been a few studies of the effect of model-order on the spatial maps of ICNs (Abou-Elseoud *et al.*, 2010), to our knowledge there is no work which studied brain function across multiple model orders. Similarly, no work has yet evaluated dynamic functional interaction jointly at multiple model orders.

## 1.3. Functional Network Connectivity (FNC): Assessment of Functional Interaction

While ICA effectively segregates the brain into ICNs, functional network connectivity (FNC) provides a way to study functional interaction and integration. FNC is defined as the temporal dependency among ICNs and commonly estimated using Pearson's correlation coefficient between ICN time courses (Jafri *et al.*, 2008). Thus, FNC characterizes the functionally integrated relationship across the brain by calculating the functional interaction between ICNs.

Traditionally, functional integration has been studied using static FNC, where the overall functional interactions are calculated using scan-length averaged FNC. However, the brain constantly integrates and processes the information in real-time. Considering the brain's rich, dynamic nature, a number of methods have moved beyond the "static" oversimplification and evaluate the temporal reconfiguration of functional interactions using dynamic FNC (Allen *et al.*, 2014; Calhoun *et al.*, 2014). The dynamic FNC approaches

calculate time-resolved FNC allowing us to study variations in functional integrations over time and identify different brain functional interaction patterns, also known as brain functional states (Iraji *et al.*, 2020a).

#### 1.4. Schizophrenia

Schizophrenia is a psychotic disorder accompanied by various cognitive impairments and a decrease in social and occupational functioning. Schizophrenia is a heterogeneous syndromic diagnosis of exclusion, lacks unique symptoms and is diagnosed clinically by both positive symptoms, such as delusions, hallucinations, disorganized speech, disorganized or catatonic behavior; and negative symptoms, such as apathy, blunted affect, and anhedonia (American Psychiatric Association, 2013), plus a decline in social functioning. Schizophrenia overlaps considerably with both schizo-affective disorder and psychotic bipolar disorder, not only symptomatically, but in terms of genetics and at the level of other biomarkers (Clementz *et al.*, 2016). The diverse temporal trajectory across individuals with SZ and the different types of clinical symptoms suggest alterations in various functional domains and brain capacity reductions to integrate information across the brain. Schizophrenia has been hypothesized as a developmental disorder of disrupted brain function, which can be characterized by functional dysconnectivity and/or changes in functional integration (Friston and Frith, 1995; Stephan *et al.*, 2006; Kahn *et al.*, 2015). Therefore, studying static and dynamic FNC can provide vital information about brain functional integration and its schizophrenia changes, potentially improving our understanding of the actual brain pathology underlying different schizophrenia subcategories. However, previous studies have not studied functional integrations across multiple spatial scales and have underappreciated differences between male and female cohorts (Damaraju *et al.*, 2014; Miller *et al.*, 2016; Iraji *et al.*, 2019a; Miller *et al.*, 2019; Faghiri *et al.*, 2020).

Schizophrenia incidence is higher in men (Aleman *et al.*, 2003; McGrath *et al.*, 2004), but paradoxically there is equal overall prevalence (Saha *et al.*, 2005). There is also evidence suggesting sex-differences in onset, symptom expression, and outcome in schizophrenia (Navarro *et al.*, 1996; Nawka *et al.*, 2013; Li *et al.*, 2016). For instance, males have more severe overall symptoms, worse outcomes, more negative and fewer affective symptoms, and experience symptoms earlier than females (Li *et al.*, 2016). Furthermore, symptoms respond more quickly to treatments in females. However, sex differences in symptoms and outcomes also depend on the age of onset and treatment (Li *et al.*, 2016; Seeman, 2019). Understanding sex-specific characteristics of functional connectivity, which is currently lacking in the field, can help

provide an important insight to understand sex differences in schizophrenia and potentially the opportunity to deliver sex-specific treatments and care for individuals with schizophrenia.

Considering the previous static and dynamic FNC findings on sex differences in typical control cohorts (Allen *et al.*, 2011; Yaesoubi *et al.*, 2020) and previous report on sex differences in schizophrenia (Navarro *et al.*, 1996; Nawka *et al.*, 2013; Li *et al.*, 2016), we hypothesize that multiscale functional interactions capture sex-specific changes in schizophrenia, which are significantly correlated with schizophrenia's symptoms score. We examined our hypothesis using the following pipeline: 1) we estimated ICNs at multiple spatial scales using ICA with model-orders of 25, 50, 75, and 100; 2) we calculated the multi-spatial scale static and dynamic functional integrations using within and between model-orders static FNC and dynamic FNC using a window-based approach (Allen *et al.*, 2014; Iraj *et al.*, 2020a); 3) we evaluated sex-specific differences between typical controls and individuals with schizophrenia.

## 2. MATERIALS AND METHODS

### 2.1. Participant Demographics and Data Selection Inclusion Criteria

The data used in this study selected from three projects, including FBIRN (Functional Imaging Biomedical Informatics Research Network), MPRC (Maryland Psychiatric Research Center), and COBRE (Center for Biomedical Research Excellence). We selected a subset of data that satisfies the inclusion criteria, including 1) data of individual with typical control or schizophrenia diagnosis; 2) data with high-quality registration to echo-planar imaging (EPI) template; and 3) the head motion transition should be less than 3° rotations and 3 mm translations in every direction (Fu *et al.*, 2020). Mean framewise displacement among selected subject is average  $\pm$  standard deviation =  $0.1778 \pm 0.1228$ ; min ~ max =  $0.0355 \sim 0.9441$ . Thus, we report on resting-state fMRI (rsfMRI) data from 827 individuals, including 477 typical controls and 350 individuals with schizophrenia selected (Table 1).

Table 1. Demographic information of the data used in the study. FBIRN: Functional Imaging Biomedical Informatics Research Network, MPRC: Maryland Psychiatric Research Center, COBRE: Center for Biomedical Research Excellence

Project	diagnostic	N	sex	N	Age (years)	
					mean $\pm$ sd	median/range
FBIRN	Control group	160	Male	115	37.26 $\pm$ 10.71	39/(19-59)
			Female	45	36.47 $\pm$ 11.33	33/(19-58)
	Schizophrenia group	150	Male	114	38.74 $\pm$ 11.78	40/(18-62)
			Female	36	39.06 $\pm$ 11.40	36/(21-57)



<b>MPRC</b>	Control group	238	Male	94	$38.72 \pm 13.63$	40/(12-68)
			Female	144	$41.22 \pm 16.06$	44/(10-79)
	Schizophrenia group	150	Male	98	$35.57 \pm 13.18$	32/(13-63)
			Female	52	$44.60 \pm 13.87$	47/(13-63)
<b>COBRE</b>	Control group	79	Male	55	$39.07 \pm 12.43$	38/(18-65)
			Female	24	$34.92 \pm 10.23$	34/(18-58)
	Schizophrenia group	50	Male	42	$37.43 \pm 15.05$	32.5/(19-64)
			Female	8	$43.25 \pm 12.78$	40/(31-65)

## 2.2. Data Acquisition

The FBIRN dataset was collected from seven sites. The same resting-state fMRI (rsfMRI) parameters were used across all sites: a standard gradient echo-planar imaging (EPI) sequence, repetition time (TR)/echo time (TE) = 2000/30 ms, voxel spacing size =  $3.4375 \times 3.4375 \times 4$  mm, slice gap = 1 mm, flip angle (FA) =  $77^\circ$ , field of view (FOV) =  $220 \times 220$  mm, and a total of 162 volume. Six of the seven sites used 3-Tesla Siemens Tim Trio scanners, and one site used a 3-Tesla General Electric Discovery MR750 scanner.

The MPRC dataset was collected in three sites using a standard EPI sequence, including Siemens 3-Tesla Siemens Allegra scanner (TR/TE = 2000/27 ms, voxel spacing size =  $3.44 \times 3.44 \times 4$  mm, FOV =  $220 \times 220$  mm, and 150 volumes), 3-Tesla Siemens Trio scanner (TR/TE = 2210/30 ms, voxel spacing size =  $3.44 \times 3.44 \times 4$  mm, FOV =  $220 \times 220$  mm, and 140 volumes), and 3-Tesla Siemens Tim Trio scanner (TR/TE = 2000/30 ms, voxel spacing size =  $1.72 \times 1.72 \times 4$  mm, FOV =  $220 \times 220$  mm, and 444 volumes).

The COBRE dataset was collected in one site using a standard EPI sequence with TR/TE = 2000/29 ms, voxel spacing size =  $3.75 \times 3.75 \times 4.5$  mm, slice gap = 1.05 mm, FA =  $75^\circ$ , FOV =  $240 \times 240$  mm, and a total of 149 volumes. Data was collected using a 3-Tesla Siemens TIM Trio scanner.

## 2.3. Preprocessing/MRI Data Preprocessing

The preprocessing was performed primarily using the statistical parametric mapping (SPM12, <http://www.fil.ion.ucl.ac.uk/spm/>) toolbox. The rsfMRI data preprocessing using the following steps: 1) discarding the first five volumes for magnetization equilibrium purposes, 2) rigid motion correction to correct subject head motion during scan, and 3) slice-time correction to account for temporally misalignment in data acquisition. Next, the data of each subject was nonlinearly registered to a Montreal Neurological Institute (MNI) echo-planar imaging (EPI) template, resampled to  $3 \text{ mm}^3$  isotropic voxels,

and spatially smoothed using a Gaussian kernel with a 6 mm full width at half-maximum (FWHM = 6 mm). The voxel time courses were then z-scored (variance normalized) to enhance sensitivity to functional segregation and functional sources (Iraji *et al.*, 2019c).

Furthermore, prior to calculating static and dynamic FNC, an additional post hoc cleaning procedure was performed on the time courses of ICNs to reduce the effect of remaining noise, which may not be wholly removed using ICA, and to improve the detection of dynamic FNC patterns (Allen *et al.*, 2014). The procedure includes 1) removing linear, quadratic, and cubic trends, 2) regressing out the six motion realignment parameters and their derivatives, 3) despiking and replacing outliers with the best estimate using a third-order spline fit to the clean portions of the time courses (Allen *et al.*, 2014), and 4) bandpass filtering using a fifth-order Butterworth filter with a cutoff frequency of 0.01 Hz-0.15 Hz.

#### 2.4. Intrinsic Connectivity Network (ICNs) Estimation

For the initial work in this paper, we utilized spatial ICA with several model orders (25, 50, 75, and 100) to identify intrinsic connectivity networks (ICNs) at multiple spatial scales. Similar to most ICA based studies of fMRI, we implemented group-level spatial ICA followed by a back-reconstruction technique to estimate subjects-specific ICs and associated time courses.

We used the GIFT toolbox (<https://trendscenter.org/software/gift/>) (Calhoun *et al.*, 2001; Calhoun and Adali, 2012; Iraji *et al.*, 2020a). First, subject-specific spatial principal components analysis (PCA) was applied to normalize the data and retain maximum subject-level variance (greater than 99.99%). All subject-level principal components were concatenated together across the time dimension, and group-level spatial PCA was applied to concatenated subject-level principal components.  $N$  (25, 50, 75, and 100) group-level principal components that explained the maximum variance were selected as the input for spatial ICA to calculate  $N$  (25, 50, 75, and 100) group independent components.

Infomax was chosen as the ICA algorithm because it has been widely used and compares favorability with other algorithms (Correa *et al.*, 2007a; Correa *et al.*, 2005). For each model-order ( $N = 25, 50, 75$ , and 100), the Infomax ICA algorithm was run 100 times using the ICASSO framework, and the most stable, reliable run was selected for future analysis (Himberg *et al.*, 2004; Ma *et al.*, 2011). Next, the subject-specific independent components time courses were calculated using the spatial multiple regression technique (Calhoun *et al.*, 2004).



We selected a subset of independent components as ICNs if they are stable (ICASSO stability index > 0.8) and depict common ICNs properties including 1) dominant low-frequency fluctuations of their time courses evaluated using dynamic range and the ratio of low frequency to high-frequency power, 2) exhibit peak activations in the gray matter, 3) have low spatial overlap with vascular, ventricular, and 4) low spatial similarity with motion and other known artifacts. Finally, ICNs were grouped into functional domains based on prior knowledge from previous studies.

## 2.5. Static and Dynamic FNC Calculation

We calculated static and dynamic functional network connectivity (FNC) between every single pair of ICNs across all model-orders to effectively capture functional integration and interaction across different spatial scales. Static FNC (sFNC) was estimated by calculating the Pearson correlation between each pair of ICNs time courses resulting in one sFNC matrix for each individual. Each element of the sFNC matrix is the functional connectivity between a pair of ICNs.

In contrast to sFNC, which uses the full length of scan, in dynamic FNC (dFNC), we calculate multiple FNC matrices for different time segments of scan (i.e., FNC matrices for durations smaller than the whole time series) (Iraji *et al.*, 2020a). As a result, we can study variations in FNC over time. Here, we used a windowed-based approach with the slide step size of two seconds and the tapered window, created by convolving a rectangle window (width = 44 seconds) with a Gaussian ( $\sigma = 6$  seconds). This results in a series of windowed-FNC matrices over time (FNC as a function of time), containing dFNC information.

Next, we identified dFNC states from windowed-FNC matrices using the k-means clustering, in which each cluster represents one dynamic state (Iraji *et al.*, 2020a). We applied a two-stage k-means clustering. First, windows with local maxima with FNC variances were selected for each subject, and k-means clustering was applied to the set of all subject-specific local maxima (also known as exemplars). We used the city-block distance metric and repeated k-means clustering 100 times with different initializations using the k-means++ technique to increase the chance of escaping local minima. The resulting centroids were then used to initialize a clustering to all 93,451 (827 subjects  $\times$  113 windows) windowed-FNC matrices. The optimal number of dFNC states was selected using the elbow criterion and running the clustering procedure for 1 to 15 clusters. Subject-specific dFNC states were next estimated by averaging windowed-FNC of time-windows assigned to a given state.

We repeated the dFNC states identification procedures using two alternative ways to ensure that the dFNC states are not biased to the clustering algorithm. 1) We first applied k-means clustering at the subject-level and then concatenated the subject-level centroids for group-level clustering and identifying dFNC states. 2) We directly applied k-mean clustering to all 93,451 (827 subjects  $\times$  113 windows) windowed-FNC matrices.

## 2.6. Group Comparison Analysis

We evaluated sex-specific differences in multiscale sFNC and dFNC between the control group (CT) and the individuals with schizophrenia (SZ). For each sex cohort, male and female, we separately assessed diagnostic group differences, i.e., male controls versus male individuals with schizophrenia (maleCT vs. maleSZ) and female controls versus female individuals with schizophrenia (femaleCT vs. femaleSZ). We used a general linear model (GLM) with age, data acquisition site, and mean framewise displacement as covariates. Framewise displacement is the sum of changes in the six rigid-body transform parameters (framewise displacement(t) =  $|\Delta dx(t)| + |\Delta dy(t)| + |\Delta dz(t)| + |\Delta \alpha(t)| + |\Delta \beta(t)| + |\Delta \gamma(t)|$ ). Mean framewise displacement was added to the GLM to account for any residual motion effect that was not removed in the previous three motion-removal steps. The statistical analysis results were corrected for multiple comparisons using a 5% false discovery rate (FDR). It is worth mentioning that all statistical analysis results were combined (sFNC and dFNC; male and female) and corrected for multiple comparisons, which is more conservative than correcting for each statistical analysis separately.

Next, we evaluated sex-specific differences for the sFNC and dFNC features that showed a significant difference between the control group and individuals with schizophrenia in either of the sex cohorts (“maleCT vs. maleSZ” and/or “femaleCT vs. females”). For each feature, we compared the difference of the  $t$ -value of GLM statistic between two sex cohorts (“ $t$ -value of maleCT vs. maleSZ” - “ $t$ -value of femaleSZ vs. femaleCT”) with a null distribution. The  $p$ -value of the  $t$ -value of difference was corrected for multiple comparisons using the same procedure explained in the previous paragraph.

The null distribution was created by randomly permuting sex labels within each diagnostic group. In other words, the diagnostic label remained intact; individuals with schizophrenia remained schizophrenia, and control subjects remained in the control group, and only the sex labels were randomly permuted. Furthermore, the number of females and males in each diagnostic group did not change. This permutation process was repeated 5000 times. For each permutation, the GLM was applied to two null male and null

female cohorts independently. For each feature, the difference of the  $t$ -value of diagnosis for two null cohorts was calculated. This results in 5000 samples of the null distribution for each feature.

We also studied sex-specific differences at the domain-level across different spatial scales. For static FNC and each dynamic state, the average FNC was calculated within and between seven functional domains both within and between four model-orders, resulting in a 27-by-27 domain-level functional integration matrix. The static and dynamic state domain-level functional integration matrices were then evaluated for sex-specific differences.

## 2.7. Relationship with Symptom Scores

We further evaluate if the multiscale functional network connectivity pairs showing sex-specific changes in schizophrenia are related to the symptoms of schizophrenia. The positive and negative syndrome scale (PANSS) scores are available for the FBIRN dataset, while the MPRC dataset includes the brief psychiatric rating scale (BPRS) scores. We transformed BPRS total scores to PANSS total scores using the matching obtained from 3767 individuals (Leucht *et al.*, 2013). Next, we evaluated the relationship between the PANSS total score and domain-level features with significant sex-specific differences. Correlation analyses were conducted after regressing out age, site, and meanFD and corrected for multiple comparisons.

## 3. RESULTS

### 3.1. Multi-Spatial Scale Functional Segregation: Intrinsic Connectivity Networks (ICNs)

We performed spatial ICA with 25, 50, 75, and 100 components on rsfMRI data from 827 subjects to functionally segregate the brain at different spatial scales. Based on the criteria explained in Section 2.4, we identified 15, 28, 36, and 48 independent components as ICNs for model orders 25, 50, 75, and 100, respectively. Detailed information of the ICNs, including spatial maps, coordinates of peak activations, and temporal and frequency information, can be found in Supplementary 1. ICNs were grouped into seven functional domains (FDs) by their anatomical and functional properties. The seven functional domains are Cognitive Control (CC), Cerebellum (CR), Default Mode (DM), Subcortical (SB), Somatomotor (SM), Temporal (TP), Visual (VS). Figure 1 illustrates the composite views of functional domains for each model order and aggregated, and Table 2 shows the number of ICNs for each model order and functional domain. The results suggest as the model order increases, the number of ICNs increases, and the brain and

the functional domains segregate into more functional sources (ICNs). For instance, the subcortical (SB) domain consists of only one ICN in model order 25, enclosing the whole subcortical regions, while it parcels into spatially distinct ICNs as model order increases. Interestingly, across different model orders, we observed ICNs with high spatial overlap (high spatial similarity) but clearly distinct features. Figure 4(R2, A) and Figure 4(R2, B) show two distinct ICNs with high spatial overlap associated with the primary motor cortex.

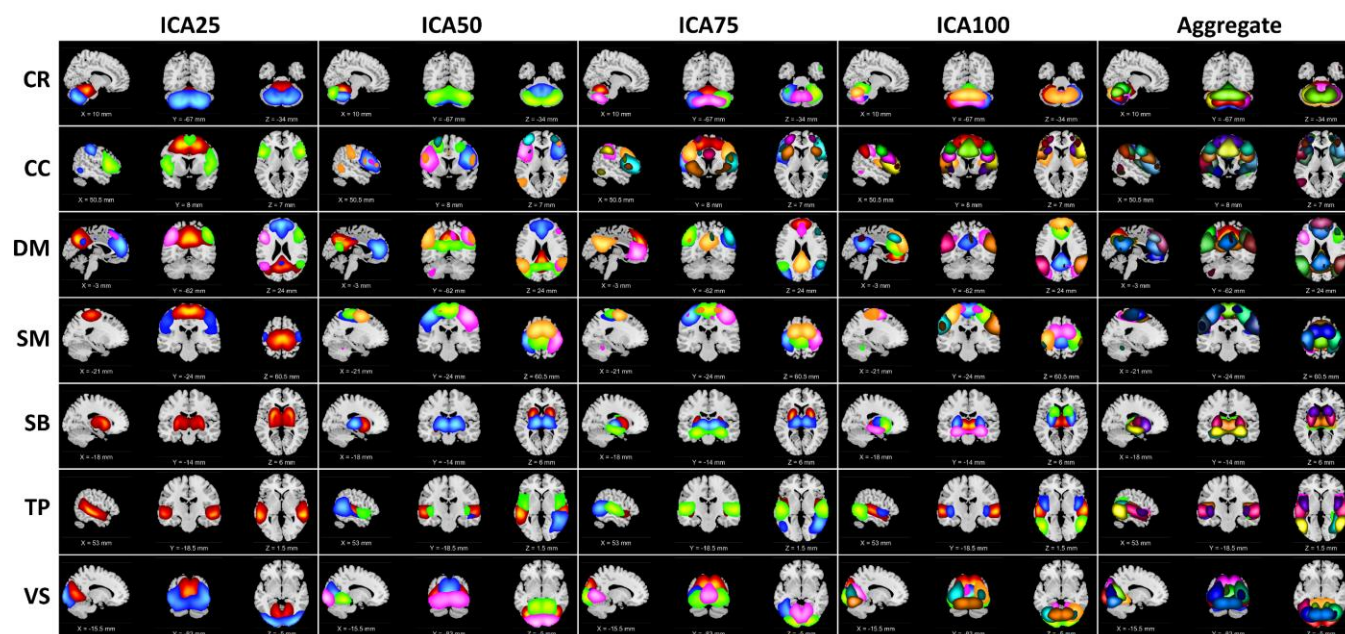


Figure 1. Visualization of the intrinsic connectivity networks (ICNs) identified from four ICA model orders of 25, 50, 75, and 100. ICNs were grouped into seven functional domains (FD) based on their anatomical and functional properties. The functional domains are Cognitive Control (CC), Default Mode (DM), Visual (VS), Subcortical (SB), Cerebellum (CR), Somatomotor (SM), and Temporal (TP). Each column shows the composite maps of seven functional domains for four ICA model orders and aggregated. Each color represents the spatial map of one ICN thresholded at  $|Z| > 1.96$  ( $p = 0.05$ ).

Table 2. The number of Intrinsic Connectivity Networks (ICNs) for each model order and functional domains, Cognitive Control (CC), Cerebellum (CR), Default Mode (DM), Subcortical (SB), Somatomotor (SM), and Temporal (TP).

	CR	CC	DM	SM	SB	TP	VS	Total
IC25	2	3	4	2	1	1	2	15
IC50	3	6	5	5	2	3	4	28
IC75	4	11	6	5	3	3	4	36
IC100	5	14	8	7	4	3	7	48
Total	14	34	23	19	10	10	17	

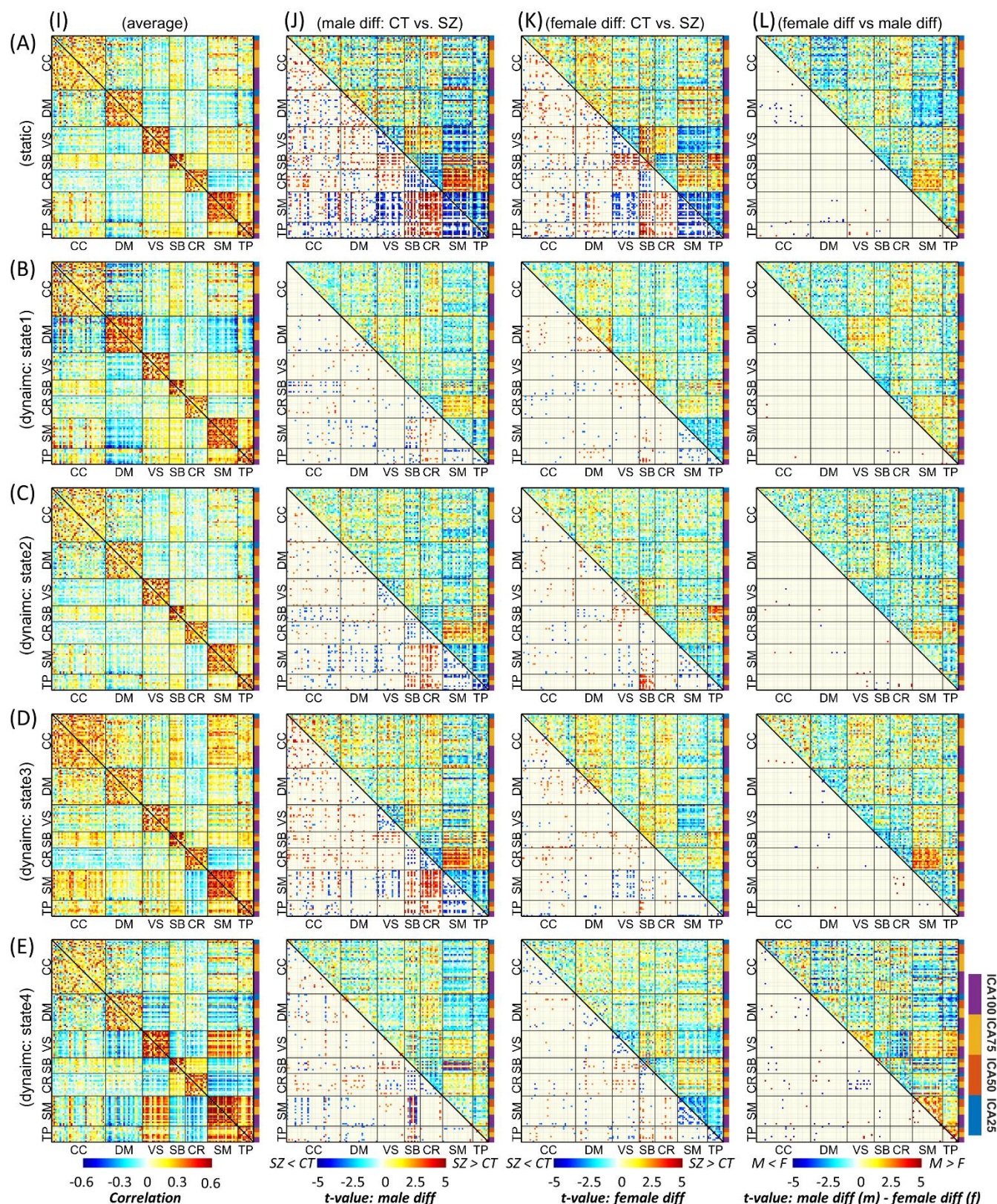
### 3.2. Dynamic Functional Integration: Static/Dynamic Functional Network Connectivity (sFNC/dFNC)

Figure 2(A, I) and Figure 3(A, I) display “block” and “finger” plots of the group-level multiscale functional integration computed using the entire scan length (i.e., static functional network connectivity (sFNC)). sFNC shows similar patterns for control groups, individuals with schizophrenia, males, and females. In the block plot, we sort ICNs by functional domain and then model order. The block plot of sFNC resembles previous single model order studies, showing modular organization within functional domains across model orders. Consistent with prior literature (Allen *et al.*, 2011), we observed an overall negative association (anticorrelation) between the default model and the rest of the brain, particularly the visual, somatomotor, and temporal domains, during rest. Interestingly, this negative association with more prominent between model orders, for example, between the default mode of model order 25 (DM25) and the somatomotor of model order 100 (SM100). We also observed strong FNC between the somatomotor, temporal, and visual domains, and between the subcortical and cerebellum domains. Figure 2 suggests that the FNC within functional domains is stronger than between functional domains, and this pattern is consistent for both within and between model orders. The similarity in FNC pattern within and between model orders can be observed in the finger plots (Figure 3), where ICNs are sorted first by model order and then functional domains. The finger plot (Figure 3) shows functional domain (FD) modular patterns (stronger FNC within FDs compared to between FDs) between model orders similar to within model order.

Focusing on brain dynamics, dynamic FNC (dFNC) analysis shows variations in FNC over time, which give rise to distinct functional integration patterns (dFNC states). The elbow criterion identified four as the optimal number of states. Figure 2 and Figure 3 show the dFNC states. These states are fully reproducible and identified using different clustering procedures (see section 2.32.5). State 1 accounts for 23.76% of all windows (percentage of occurrences, POC = 23.76%), and it is dominated by a strong anticorrelation pattern between the default mode and other functional domains, which can be related to the role of the default mode in reconciling information and subserve the baseline mental activity. State 2 (POC = 38.3%) is distinct by weaker FNC, particularly weaker between functional domains potentially representing the brain's global segregation state. In contrast, State 3 (POC = 21.31%) demonstrates overall positive FNC across the cerebral cortex, potentially representing global functional integration. Of particular note, the cerebellum shows overall negative FNC with cerebral functional domains in State 3. The negative association between the cerebellar domain and sensorimotor functional domains is prominent in state 4 with POC = 16.60%. State 4 can be distinguished with strong functional integration

1 between the visual, somatomotor, and temporal domains, and their anticorrelation patterns with the rest  
2 of the brain. This state also shows strong functional integration between the subcortical and cerebellar  
3 domains.







FNC states. Column *J* shows the result of group comparison between male individuals with schizophrenia (SZ) and the male control group (CT). Column *K* shows the result of group comparison between SZ and CT individuals in the female cohort. In columns *J* and *K*, the upper triangular shows the *t*-value of statistical comparisons, and the lower triangular shows statistically significant differences after FDR correction for multiple comparisons (FDR-corrected threshold = 0.05). Column *L* shows the result of the statistical comparison between the differences observed in the male cohort versus the female cohort. The upper triangular in shows the differences between the *t*-value of statistical comparisons in male and female cohorts (“*t*-value of maleSZ vs. maleCT” - “*t*-value of femaleSZ vs. femaleCT”), and the lower triangular shows the SZ-associated abnormal patterns that are significantly different between male and female cohorts after FDR correction. Cognitive Control (CC), Default Mode (DM), Visual (VS), Subcortical (SB), Cerebellum (CR), Somatomotor (SM), and Temporal (TP).

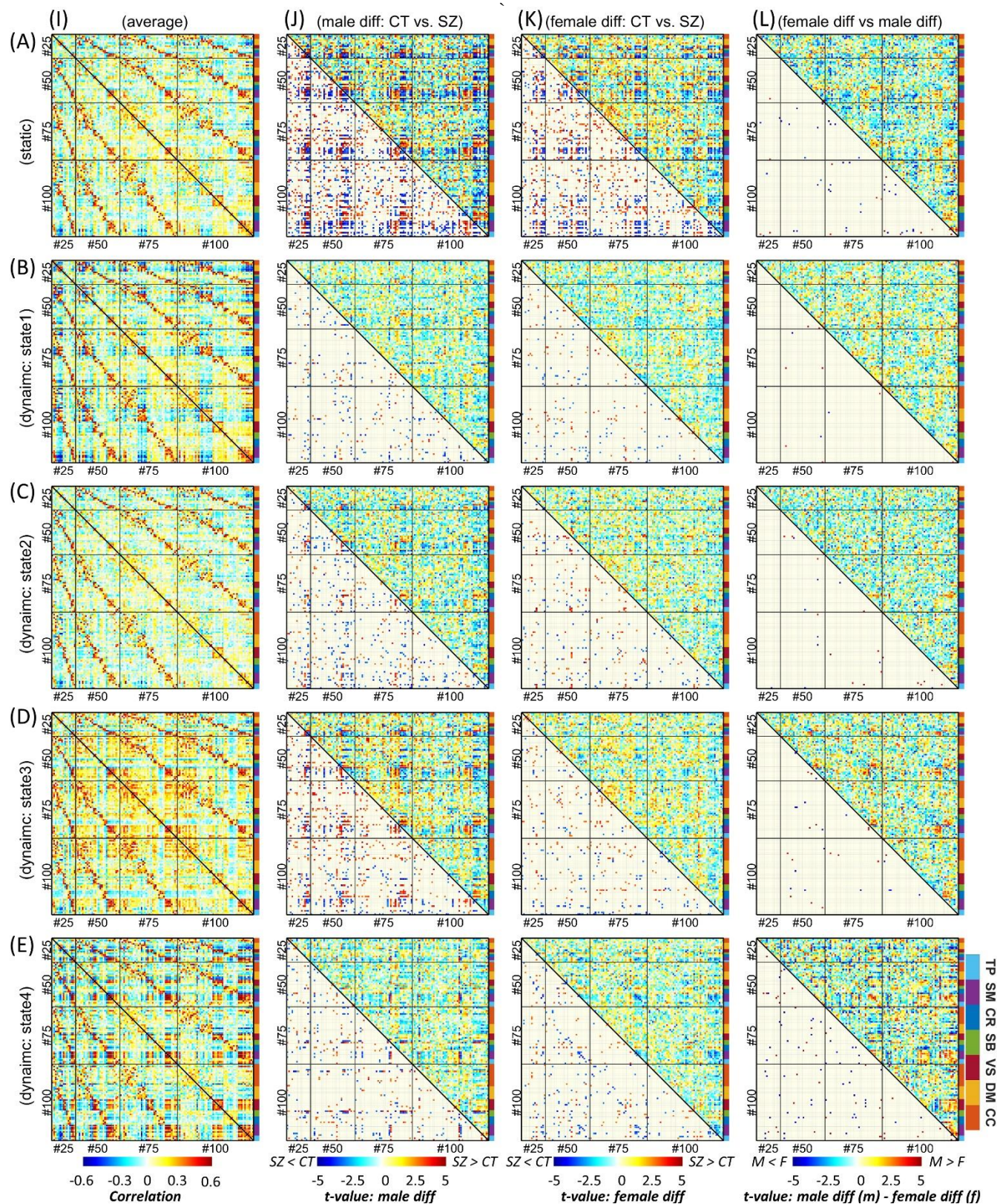


Figure 3. Finger plot of multiscale functional integration. ICNs are sorted by model order then functional domain. Row A is the result of static FNC analysis, and rows B to E represent the four dynamic states. Column I is the average FNC matrix for static FNC and dynamic



FNC states. Column *J* shows the result of group comparison between male individuals with schizophrenia (SZ) and the male control group (CT). Column *K* shows the result of group comparison between SZ and CT individuals in the female cohort. In columns *J* and *K*, the upper triangular shows the *t*-value of statistical comparisons, and the lower triangular shows statistically significant differences after FDR correction for multiple comparisons (FDR-corrected threshold = 0.05). Column *L* shows the result of the statistical comparison between the differences observed in the male cohort versus the female cohort. The upper triangular in shows the differences between the *t*-value of statistical comparisons in male and female cohorts (“*t*-value of maleSZ vs. maleCT” - “*t*-value of femaleSZ vs. femaleCT”), and the lower triangular shows the SZ-associated abnormal patterns that are significantly different between male and female cohorts after FDR correction. Cognitive Control (CC), Default Mode (DM), Visual (VS), Subcortical (SB), Cerebellum (CR), Somatomotor (SM), and Temporal (TP).

### 3.3. Sex-Specific Differences in Individuals with Schizophrenia

Multiscale functional integration was further studied by evaluating sex-specific differences in multiscale sFNC and dFNC between the control group (CT) and the individuals with schizophrenia (SZ). In Figure 2 and Figure 3, columns *J* and *K* show the statistical analysis for each sex cohort using a general linear model (GLM) with age, data acquisition site, and mean framewise displacement as covariates.

In general, sFNC shows more differences between SZ and CT in both sex cohorts than each dFNC state individually; however, the total number of tests that survived FDR correction is comparable between sFNC (Supplementary 2). In the female cohort, 576 FNC pairs show significant differences in both sFNC and dFNC, while we identified 638 and 402 FNC pairs show significant differences only in sFNC and dFNC, respectively. In the male cohort, the number of FNC pairs that show significant differences in both sFNC and dFNC is 1076, and the numbers of FNC pairs that show significant differences only in sFNC and dFNC are 720 and 640, respectively. Furthermore, dFNC analysis shows that in the female (male) cohort, 790 (1246) and 3 (21) FNC pairs, respectively, show significant differences in only one dynamic state and all four dynamic states.

Individuals with schizophrenia show reduced sFNC strength within and between the SM and TP domains in male and female cohorts. Looking at dFNC results, we observed these differences emerge in different states for male and female cohorts, i.e., mainly in State 3 for the male cohort and State 4 for females. We observed the sex-specific differences in the SM and TP domains are more pronounced in dFNC states, particularly in State 4. Individuals with SZ also have weaker sFNC and dFNC within the VS and between VS domain and SM and TP domains. Furthermore, with a few exceptions, we observed an overall sFNC and dFNC increases between the SB and the CR, on the one hand, and the SM, the TP, and the VIS on the other hand. We observed the strongest sex-specific differences in State 4 between the VS and the CR.

1 The results also show significant differences between male and female cohorts across other functional  
2 domains in both sFNC and dFNC. For instance, the sFNC between the CC and DMN significant  
3 differences in SZ-related alterations between male and female cohorts.

4 The sex-specific differences are more prevalent in State 4 than sFNC and other dynamic states  
5 (Supplementary 2). The number of FNC pairs that show significant sex differences in both sFNC and  
6 dFNC is only nine. The results also suggest the largest sex-specific changes in schizophrenia are mainly  
7 observed in the dFNC state 4, and they belong to between model-order FNC (Figure 4). Interestingly, we  
8 observed opposite patterns of alterations for male and female cohorts in several significant differences.  
9 For instance, Figure 4(R1, D4) shows significant differences in the dFNC state 4 (D4) in both male (C2)  
10 and female (C3) cohorts. However, while in the male cohort, the strength of dFNC in state 4 reduced in  
11 SZ ( $t$ -value = -3.32), in the female cohort, the strength of FNC increased in SZ cohort ( $t$ -value = 3.65)  
12 compared to control group.

13 One of the advantages of using msICA is that it allows us to see how the same region can contribute to  
14 different ICNs at different spatial scales and how the functional connectivity between these ICNs varies  
15 across different populations (Figure 4(R2)).

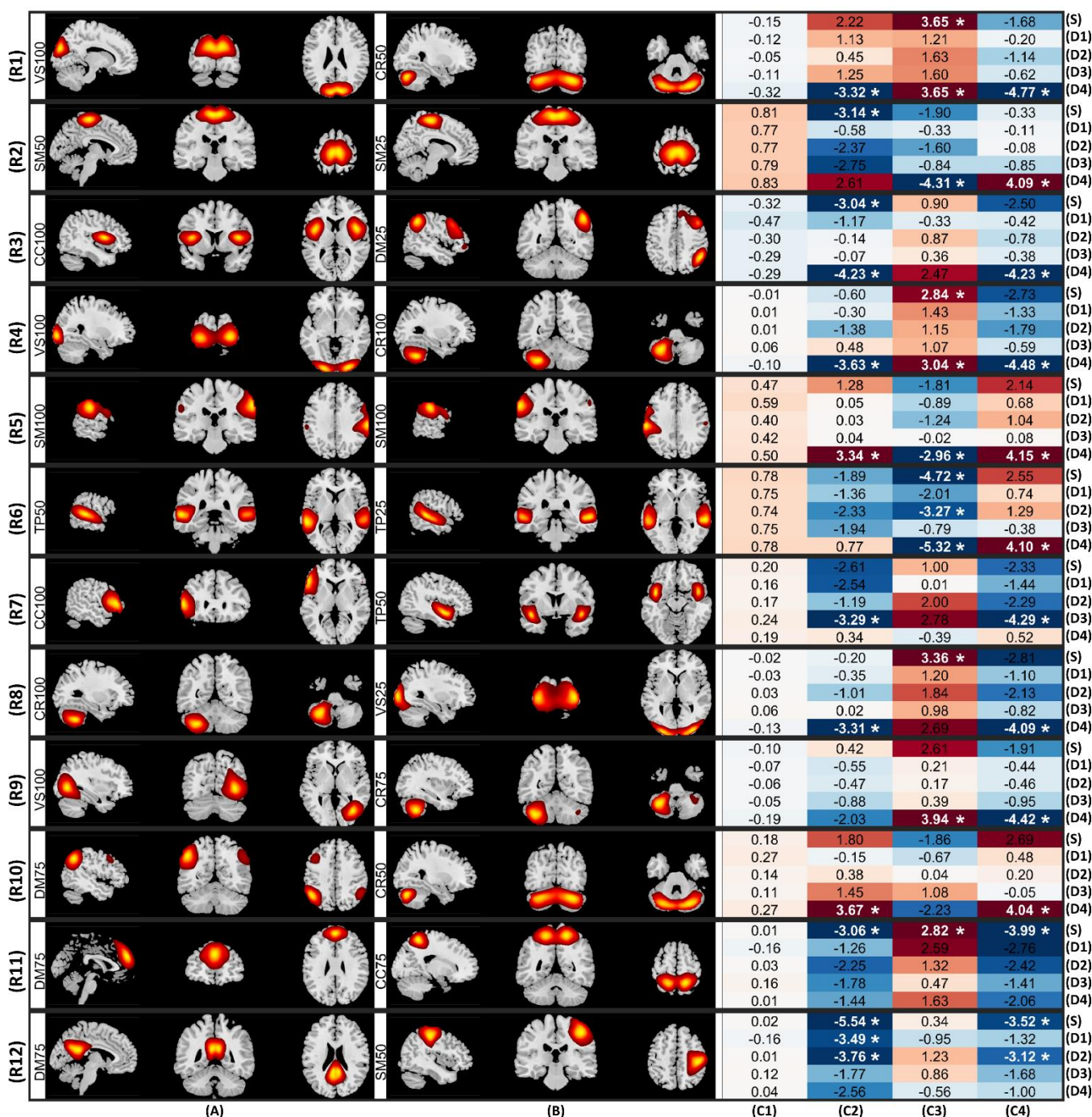


Figure 4. Static and dynamic functional network connectivity (sFNC/dFNC) pairs that show the largest sex-specific multiscale changes in schizophrenia. (S) represents the results of sFNC, and (D1) to (D4) show the results of dFNC for dynamic state 1 to 4, respectively. (A) and (B) display the sagittal, coronal, and axial views of the peak activation of intrinsic connectivity networks (ICNs) associated with each FNC pair. (C1) is the FNC strength. (C2) indicates the t-value of statistical comparisons between typical control and individual with schizophrenia in male cohort. Positive (negative) values indicate stronger (weaker) sFNC/dFNC in individuals with schizophrenia (SZ) compared to the control group. (C3) represents the t-value of statistical comparisons between typical control and individual with schizophrenia in the female cohort, where positive and negative values indicate the same pattern as (C2). (C4) shows the t-value of comparing Schizophrenia-related changes between male and female cohorts (“t-value of maleSZ vs. maleCT” - “t-value of femaleSZ vs.



1 femaleCT"). Asterisk sign \* indicates the statistical comparisons that survived multiple comparisons (5% false discovery rate, FDR).  
2 Cognitive Control (CC), Default Mode (DM), Visual (VS), Subcortical (SB), Cerebellum (CR), Somatomotor (SM), and Temporal (TP).  
3 The number after functional domain abbreviation is the model number; for example, DM25 means the default model domain from ICA  
4 model order 25.

5 Investigating sex-specific differences at the domain-level across different spatial scales, we observed sex-  
6 specific differences are more prominent in the dFNC compared to sFNC. Significant differences exist  
7 within the subcortical domain between model order 75 and 100 (SB75-SB100) in sFNC and dFNC state  
8 1 (Figure 5). State 2 shows sex-specific differences between the subcortical and temporal domains within  
9 and between several model-orders (Figure 5). State 3, on the other hand, shows sex-specific differences  
10 between the cerebellar and somatomotor across different model orders (Figure 5). Like ICN-level  
11 comparison, dynamic state 4 reveals the most sex-specific differences, including the temporal, visual, and  
12 default mode domains.

13 While sex-specific differences show stronger effects of schizophrenia in males (male diff – female diff >  
14 0) for functional domain connectivity associated with the SM and the VIS, we observe the opposite pattern  
15 for the rest of the differences. One exception is the within temporal domain functional connectivity  
16 between model order 25 and 50 in the dFNC state 4.

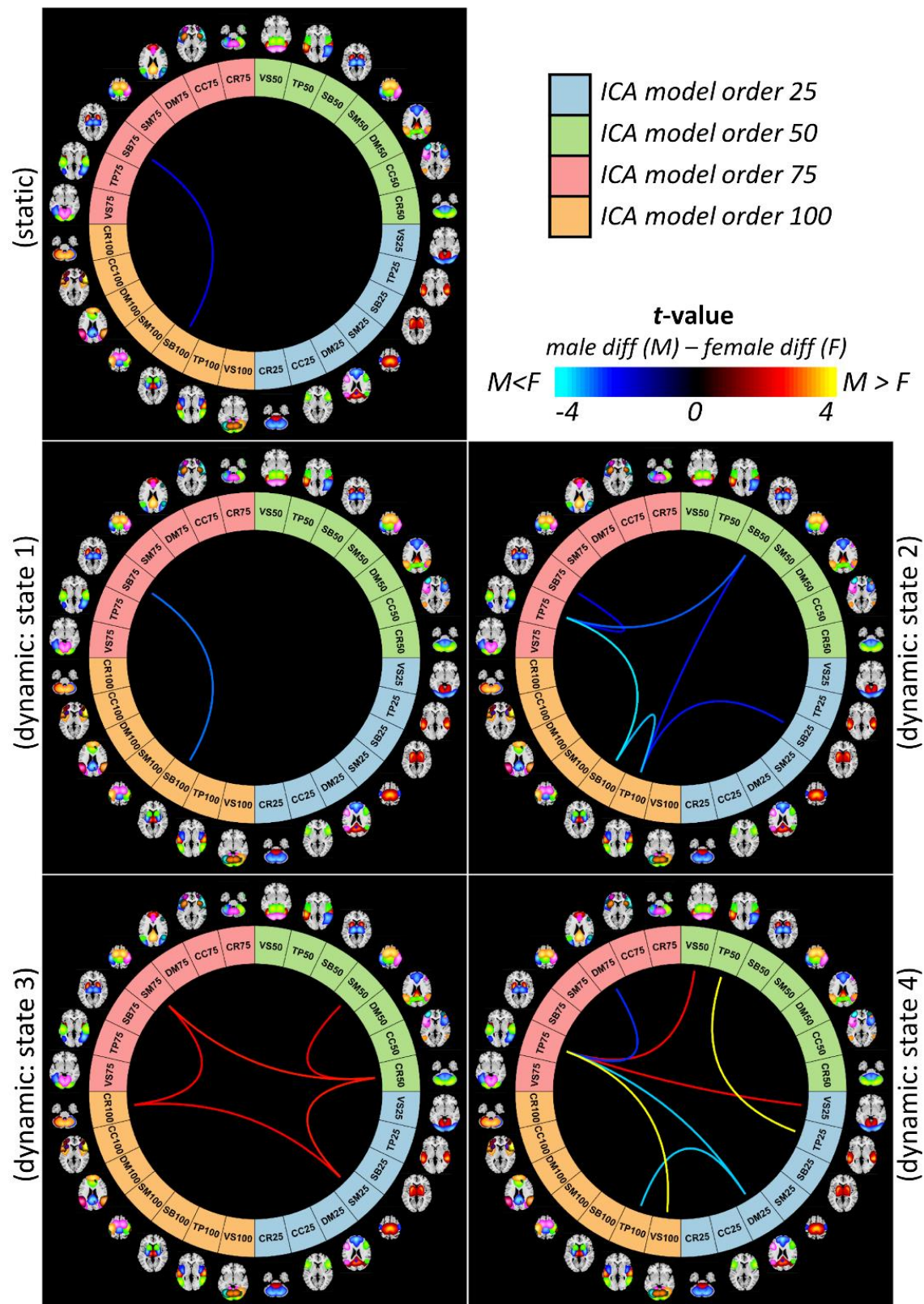


Figure 5. Sex-specific differences at the domain-level across different spatial scales. Cognitive Control (CC), Default Mode (DM), Visual (VS), Subcortical (SB), Cerebellum (CR), Somatomotor (SM), and Temporal (TP). The number after functional domain abbreviation is the model number; for example, DM25 means the default model domain from ICA model order 25.

For sex-specific changes at the domain level, we also evaluated the correlation with the PANSS total score. We observed strong correlations with  $p$ -value  $< 0.05$  in the male but not the female cohorts for four domain-level features. They include (1&2) within the subcortical domain between model order 75 and 100 (SB75-SB100) in sFNC with the correlation values of 0.281/-0.117 (male/female) and dFNC state 1 with the correlation values of 0.173/-0.197 (male/female); (3) within the temporal domain between model order 25 and 50 (TP25-TP50) in dFNC state 4 with the correlation values of 0.277/-0.062 (male/female); and (4) between the visual domain model order 25 and the temporal domain model order 75 (VS25-TP75) in dFNC state 4 with the correlation values of -0.300/-0.024 (male/female). Among these, SB75-SB100 (sFNC) and VS25-TP75 (dFNC state 4) survived multiple comparison corrections.

## 4. DISCUSSION

### 4.1. Multiscale Dynamic Interactions: Functional Segregation and Integration

Studying brain functional connectivity has improved our understanding of brain functions and the impact of brain disorders. However, currently, studying functional connectivity overwhelmingly disregard the functional connectivity across multiple spatial scales. Existing studies, at best, apply data-driven approaches like ICA to study functional interactions at single model order but overlook the FNC within and between multiple spatial scales, while the majority of them uses fixed anatomical locations of the same size (e.g., a sphere with the same radius), which in addition to disregarding multiple spatial scales interaction, they ignore differences in the spatial distribution of functional sources.

In this work, we present an approach to study multi-spatial scale dynamic functional interactions, i.e., dynamic changes that occur within and among different spatial scales, a topic that has been overlooked by the field. We leveraged the approach to study schizophrenia's alterations and its sex-specific differences, which has also been understudied as most schizophrenia research only focuses on single spatial scale FC and non-sex specific alterations of schizophrenia.

### 4.2. Multiscale ICA (msICA)

Our results show that multiscale ICA (msICA) using the Infomax algorithm is an effective, adaptive tool to identify functional sources at multiple spatial scales. Higher model order ICAs segregate the brain and functional domains into more ICNs with, in general, higher spatial granularity. For instance, the subcortical domain splits into more ICNs as the model order increases from 25 to 100. However, ICA

does not enforce a limitation on each ICN's spatial extent. Instead, ICA considers the multivariate association in the BOLD signal to segment the brain. As a result, while some functional domains break into more ICNs as the model order increases, others demonstrate a smaller amount of changes in the number of ICNs and their spatial distributions across model-orders studies in this work. For example, we observe significant changes in the ICNs associated with the cognitive control domain across model orders, particularly between model order 50 and 75, while the number of ICNs are the same for model order 50 and 75 for the somatomotor and visual domains.

Furthermore, msICA captures the multifunctionality of brain regions and identify distinct ICNs with high spatial overlap (For example, see Figure 4(R2, A) and Figure 4(R2, B)). Additional studies are needed to evaluate neurophysiological basis explaining these variations. Furthermore, in this study, we focus on only four model orders of 25, 50, 75, and 100. Future studies should reduce the incremental steps and increase the range of model orders to effectively capture ICNs associated with a larger number of spatial levels of functional hierarchy (Iraji *et al.*, 2019c). Recently, we used 1K-ICA, ICA with a model order of 1000, to parcel the brain into very fine-grained functional sources (Iraji *et al.*, 2019b). Furthermore, developing techniques that simultaneously estimates ICNs for multiple model-orders can improve the estimation of ICNs across multiple scales. Finally, considering the recent findings on spatial dynamics (Iraji *et al.*, 2019a; Iraji *et al.*, 2019c; Iraji *et al.*, 2020b), future works should also consider spatial dynamic functional segregations as the spatial patterns of functional sources may vary over time.

### 4.3. Multi-Spatial Scale dFNC

A window-based dFNC approach (Allen *et al.*, 2014; Iraji *et al.*, 2020a) was adopted to characterize the multi-spatial scale dynamic functional interactions. To our best knowledge, this is the first study that looks at sFNC/dFNC across multiple mode orders. While we observe consistency and similarity of sFNC/dFNC both within- and between-model orders, there are also distinct differences in FNC patterns across FNC patterns. The differences are more distinguishable when there are larger differences in model-orders, e.g., between model orders 25 and 100 (see, for example, Figure 3 (A), (B), and (E)). This further highlights the importance of including a wider range of model-orders in future studies.

Another important point is how we identify dFNC states. In this study, dFNC states were identified using all 127 ICNs; however, the brain may experience different states and/or temporal changes across different spatial scales. Higher functional hierarchy levels have less homogeneity and more dynamic behavior (Iraji

*et al.*, 2019c). Therefore, we expect more dynamism in the low-model order ICAs. A future study should investigate variation in dFNC states and their timing across multiple model orders and differentiate between global and state-specific dFNC states.

Furthermore, similar to multi-spatial scales, brain functional segregation and integration can occur at different temporal scales and frequencies; thus, future studies can benefit from multi-temporal scale functional interactions (Faghiri *et al.*, 2020). Developing multi-spatiotemporal scale analytic approaches and methodological framework to study functional sources is a crucial future avenue of investigation.

#### 4.4. Schizophrenia

We further investigated the advantage of multi-spatial scale analysis in schizophrenia and identifying sex-specific changes. Our results suggest disruptions in sFNC/dFNC across functional domains. Compared with controls, individuals with schizophrenia show reduced sFNC/dFNC within and between the visual, somatomotor, and temporal domains in both male and female cohorts (Figure 2). Previous studies that looked at differences between typical controls and individuals with schizophrenia also report hypoconnectivity across these functional domains using various approaches (Anticevic *et al.*, 2014; Damaraju *et al.*, 2014; Kim *et al.*, 2014; Shinn *et al.*, 2015; Iraj *et al.*, 2019a; Iraj *et al.*, 2019c; Faghiri *et al.*, 2020). Our study both confirms and extends previous findings and identifies significant differences between males and females in several FNC pairs, mainly showing larger schizophrenia-related changes in males than female cohorts. Greater SZ-related changes across these domains in males are also present at the domain level in dFNC State 4 within the temporal domain and between the temporal and visual domains (Figure 5).

Individuals with schizophrenia show hyperconnectivity of the subcortical domain with the visual, somatomotor, and temporal domains with notable exceptions in dFNC State 4. Unlike sFNC and dFNC in other states, dFNC State 4 has an overall negative association between the subcortical and the visual, somatomotor, and temporal domains (Figure 2). Certainly, temporal lobe anatomical and functional differences have been linked repeatedly to the expression of positive symptoms in schizophrenia (Barta *et al.*, 1990; Shenton *et al.*, 1992; Woodruff *et al.*, 1997). We also observe different patterns of schizophrenia-related changes in male and female cohorts. dFNC State 4 also shows distinct sex-specific differences in the cerebellum domain connectivity patterns, where we observe the opposite pattern of alterations, particularly between the cerebellum and visual domain in the male and female cohorts (Figure



2). Cerebellar dysconnectivity patterns have been linked to negative symptom expression in schizophrenia (Brady *et al.*, 2019).

The domain-level analysis suggests that major sex-dependent schizophrenia alterations at a large scale are mainly associated with the subcortical, cerebellar, temporal, and motor domains. Interestingly, most of the sex-specific differences were observed between model-order and associated with dFNC states, highlighting the importance of multiscale dynamic analysis (Figure 3 and Figure 5).

While changes in the connectivity patterns in our findings are aligned with previous schizophrenia studies, our distinct findings in sex-specific differences and distinct dFNC patterns in State 4 demand further investigations into the multi-spatial scale dFNC and sex differences in SZ. Particularly, future longitudinal studies might be used to further study the role of the age of onset on the sex-specific differences in schizophrenia and evaluate the relationship between age of onset and sex-specific differences over time.

#### **4.5. Biomarker and Importance of Sex-Specific Characteristics**

According to NIH Biomarkers Definitions Working Group, a biomarker is defined as “a characteristic that is objectively measured and evaluated as an indicator of normal biological processes, pathogenic processes, or pharmacologic responses to a therapeutic intervention (Biomarkers Definitions Working Group, 2001)”. As such, a diagnostic biomarker is defined as a characteristic or feature capable of detecting or confirming the presence of a (subtype of) disease or condition of interest (Califf, 2018). At the same time, numerous studies have observed sex differences in schizophrenia, including in the age of onset, in experiencing negative and positive symptoms, and in response to treatments (Nawka *et al.*, 2013; Li *et al.*, 2016; Seeman, 2019). Therefore, the biomarkers for schizophrenia might be somewhat different for males and females.

This study's premise is that sex influences differences in schizophrenia characteristics, and we introduce a dynamic multi-spatial scale framework to obtain candidates for sex-specific biomarkers from rsfMRI data. We observed significant sex-specific differences across several functional domains, including in subcortical and temporal connectivity patterns, which also significantly correlate with symptom scores in males but not females. Interestingly, the affected functional domains have been frequently reported to be altered in SZ and touted as having potential to serve as identifying biomarkers. Our results suggest that sex-specific functional connectivity changes might be related to schizophrenia symptoms and underlying causes and emphasize the importance of carefully incorporating sex in the development of



diagnostic/predictive/monitoring biomarkers. While sex and schizophrenia can be identified straightforwardly, there has been very little work looking at sex and schizophrenia differences across different spatial scales in resting fMRI data. The incorporation of sex as a biological variable within the context of schizophrenia may help shed new light on the neurobiological mechanisms of schizophrenia and in particular. Future studies should leverage these findings and incorporate sex into feature selection and classification algorithms to identify a set of sensitive schizophrenia-related features for use in updating nosological categories and building diagnostic and predictive models.

## 5. CONCLUSION

Brain dynamic functional interaction can occur at different spatial scales, which has been underappreciated. In this work, we propose an approach that uses multiscale ICA and dFNC to study brain function at different spatial scales. This results in a more comprehensive map of functional interactions across the brain. The not only solves the limitation of using fixed anatomical locations but also eliminates the need for model-order selection in ICA analysis. Therefore, we propose multiscale ICA (msICA), and future multi-spatial methods should be broadly applied in future studies. Going forward we can further improve the proposed approach by incorporating explicit spatial dynamics and multi-temporal scale features of functional sources. We leverage the proposed approach to study male/female common and unique aspects of sFNC/dFNC in schizophrenia, which has not been investigated despite previous reports on sex differences on the prevalence, symptoms, and responses to treatment. The majority of sex-specific differences occur in between-model-order and associated with dFNC states, further highlighting our proposed approach's benefit. Future studies are needed to validate our findings and evaluate the further benefits of multiscale analysis.

## 6. REFERENCES

- Abou-Elseoud, A., Starck, T., Remes, J., Nikkinen, J., Tervonen, O. & Kiviniemi, V. (2010) 'The effect of model order selection in group PICA', *Hum Brain Mapp*, **31**(8), pp. 1207-1216.
- Aleman, A., Kahn, R. S. & Selten, J. P. (2003) 'Sex differences in the risk of schizophrenia: evidence from meta-analysis', *Arch Gen Psychiatry*, **60**(6), pp. 565-571.
- Allen, E. A., Damaraju, E., Plis, S. M., Erhardt, E. B., Eichele, T. & Calhoun, V. D. (2014) 'Tracking whole-brain connectivity dynamics in the resting state', *Cereb Cortex*, **24**(3), pp. 663-676.
- Allen, E. A., Erhardt, E. B., Damaraju, E., Gruner, W., Segall, J. M., Silva, R. F., Havlicek, M., Rachakonda, S., Fries, J., Kalyanam, R., Michael, A. M., Caprihan, A., Turner, J. A., Eichele, T.,

- 1 Adelsheim, S., Bryan, A. D., Bustillo, J., Clark, V. P., Feldstein Ewing, S. W., Filbey, F., Ford, C. C.,  
2 Hutchison, K., Jung, R. E., Kiehl, K. A., Kodituwakku, P., Komesu, Y. M., Mayer, A. R., Pearlson, G. D.,  
3 Phillips, J. P., Sadek, J. R., Stevens, M., Teuscher, U., Thoma, R. J. & Calhoun, V. D. (2011) 'A baseline  
4 for the multivariate comparison of resting-state networks', *Front Syst Neurosci*, **5**, p. 2.
- 5 American Psychiatric Association (2013) *Diagnostic and statistical manual of mental disorders (DSM-*  
6 *5®)*, American Psychiatric Pub.
- 7 Anticevic, A., Cole, M. W., Repovs, G., Murray, J. D., Brumbaugh, M. S., Winkler, A. M., Savic, A.,  
8 Krystal, J. H., Pearlson, G. D. & Glahn, D. C. (2014) 'Characterizing thalamo-cortical disturbances in  
9 schizophrenia and bipolar illness', *Cereb Cortex*, **24**(12), pp. 3116-3130.
- 10 Barta, P. E., Pearlson, G. D., Powers, R. E., Richards, S. S. & Tune, L. E. (1990) 'Auditory hallucinations  
11 and smaller superior temporal gyral volume in schizophrenia', *Am J Psychiatry*, **147**(11), pp. 1457-1462.
- 12 Biomarkers Definitions Working Group (2001) 'Biomarkers and surrogate endpoints: preferred definitions  
13 and conceptual framework', *Clin Pharmacol Ther*, **69**(3), pp. 89-95.
- 14 Brady, R. O., Jr., Gonsalvez, I., Lee, I., Öngür, D., Seidman, L. J., Schmahmann, J. D., Eack, S. M.,  
15 Keshavan, M. S., Pascual-Leone, A. & Halko, M. A. (2019) 'Cerebellar-Prefrontal Network Connectivity  
16 and Negative Symptoms in Schizophrenia', *Am J Psychiatry*, **176**(7), pp. 512-520.
- 17 Calhoun, V. D. & Adali, T. (2012) 'Multisubject independent component analysis of fMRI: a decade of  
18 intrinsic networks, default mode, and neurodiagnostic discovery', *IEEE Rev Biomed Eng*, **5**, pp. 60-73.
- 19 Calhoun, V. D., Adali, T., Pearlson, G. D. & Pekar, J. J. (2001) 'A method for making group inferences  
20 from functional MRI data using independent component analysis', *Hum Brain Mapp*, **14**(3), pp. 140-151.
- 21 Calhoun, V. D., Miller, R., Pearlson, G. & Adali, T. (2014) 'The chronnectome: time-varying connectivity  
22 networks as the next frontier in fMRI data discovery', *Neuron*, **84**(2), pp. 262-274.
- 23 Calhoun, V. D., Pekar, J. J. & Pearlson, G. D. (2004) 'Alcohol intoxication effects on simulated driving:  
24 exploring alcohol-dose effects on brain activation using functional MRI', *Neuropsychopharmacology*,  
25 **29**(11), pp. 2097-2017.
- 26 Califf, R. M. (2018) 'Biomarker definitions and their applications', *Exp Biol Med (Maywood)*, **243**(3), pp.  
27 213-221.
- 28 Clementz, B. A., Sweeney, J. A., Hamm, J. P., Ivleva, E. I., Ethridge, L. E., Pearlson, G. D., Keshavan,  
29 M. S. & Tamminga, C. A. (2016) 'Identification of Distinct Psychosis Biotypes Using Brain-Based  
30 Biomarkers', *Am J Psychiatry*, **173**(4), pp. 373-384.
- 31 Damaraju, E., Allen, E. A., Belger, A., Ford, J. M., McEwen, S., Mathalon, D. H., Mueller, B. A., Pearlson,  
32 G. D., Potkin, S. G., Preda, A., Turner, J. A., Vaidya, J. G., van Erp, T. G. & Calhoun, V. D. (2014)  
33 'Dynamic functional connectivity analysis reveals transient states of dysconnectivity in schizophrenia',  
34 *Neuroimage Clin*, **5**, pp. 298-308.
- 35 Faghiri, A., Iraj, A., Damaraju, E., Turner, J. & Calhoun, V. D. (2020) 'A unified approach for  
36 characterizing static/dynamic connectivity frequency profiles using filter banks', *Network Neuroscience*,  
37 pp. 1-51.
- 38 Friston, K. J. & Frith, C. D. (1995) 'Schizophrenia: a disconnection syndrome?', *Clin Neurosci*, **3**(2), pp.  
39 89-97.

- 1 Fu, Z., Iraj, A., Turner, J. A., Sui, J., Miller, R., Pearlson, G. D. & Calhoun, V. D. (2020) 'Dynamic State  
2 with Covarying Brain Activity-Connectivity: On the Pathophysiology of Schizophrenia', *Neuroimage*, p.  
3 117385.
- 4 Genon, S., Reid, A., Langner, R., Amunts, K. & Eickhoff, S. B. (2018) 'How to Characterize the Function  
5 of a Brain Region', *Trends Cogn Sci*, **22**(4), pp. 350-364.
- 6 Himberg, J., Hyvarinen, A. & Esposito, F. (2004) 'Validating the independent components of  
7 neuroimaging time series via clustering and visualization', *Neuroimage*, **22**(3), pp. 1214-1222.
- 8 Iraj, A., Calhoun, V. D., Wiseman, N. M., Davoodi-Bojd, E., Avanaki, M. R. N., Haacke, E. M. & Kou,  
9 Z. (2016) 'The connectivity domain: Analyzing resting state fMRI data using feature-based data-driven  
10 and model-based methods', *Neuroimage*, **134**, pp. 494-507.
- 11 Iraj, A., Deramus, T. P., Lewis, N., Yaesoubi, M., Stephen, J. M., Erhardt, E., Belger, A., Ford, J. M.,  
12 McEwen, S., Mathalon, D. H., Mueller, B. A., Pearlson, G. D., Potkin, S. G., Preda, A., Turner, J. A.,  
13 Vaidya, J. G., van Erp, T. G. M. & Calhoun, V. D. (2019a) 'The spatial chronnectome reveals a dynamic  
14 interplay between functional segregation and integration', *Hum Brain Mapp*, **40**(10), pp. 3058-3077.
- 15 Iraj, A., Faghiri, A., Lewis, N., Fu, Z., DeRamus, T., Qi, S., Rachakonda, S., Du, Y. & Calhoun, V.  
16 (2019b) *Ultra-high-order ICA: an exploration of highly resolved data-driven representation of intrinsic  
17 connectivity networks (sparse ICNs)*, SPIE.
- 18 Iraj, A., Faghiri, A., Lewis, N., Fu, Z., Rachakonda, S. & Calhoun, V. D. (2020a) 'Tools of the trade:  
19 Estimating time-varying connectivity patterns from fMRI data', *Soc Cogn Affect Neurosci*.
- 20 Iraj, A., Fu, Z., Damaraju, E., DeRamus, T. P., Lewis, N., Bustillo, J. R., Lenroot, R. K., Belger, A., Ford,  
21 J. M., McEwen, S., Mathalon, D. H., Mueller, B. A., Pearlson, G. D., Potkin, S. G., Preda, A., Turner, J.  
22 A., Vaidya, J. G., van Erp, T. G. M. & Calhoun, V. D. (2019c) 'Spatial dynamics within and between brain  
23 functional domains: A hierarchical approach to study time-varying brain function', *Hum Brain Mapp*,  
24 **40**(6), pp. 1969-1986.
- 25 Iraj, A., Miller, R., Adali, T. & Calhoun, V. D. (2020b) 'Space: A Missing Piece of the Dynamic Puzzle',  
26 *Trends Cogn Sci*, **24**(2), pp. 135-149.
- 27 Jafri, M. J., Pearlson, G. D., Stevens, M. & Calhoun, V. D. (2008) 'A method for functional network  
28 connectivity among spatially independent resting-state components in schizophrenia', *Neuroimage*, **39**(4),  
29 pp. 1666-1681.
- 30 Kahn, R. S., Sommer, I. E., Murray, R. M., Meyer-Lindenberg, A., Weinberger, D. R., Cannon, T. D.,  
31 O'Donovan, M., Correll, C. U., Kane, J. M., van Os, J. & Insel, T. R. (2015) 'Schizophrenia', *Nat Rev Dis  
32 Primers*, **1**, p. 15067.
- 33 Kim, D. J., Kent, J. S., Bolbecker, A. R., Sporns, O., Cheng, H., Newman, S. D., Puce, A., O'Donnell, B.  
34 F. & Hetrick, W. P. (2014) 'Disrupted modular architecture of cerebellum in schizophrenia: a graph  
35 theoretic analysis', *Schizophr Bull*, **40**(6), pp. 1216-1226.
- 36 Leucht, S., Rothe, P., Davis, J. M. & Engel, R. R. (2013) 'Equipercntile linking of the BPRS and the  
37 PANSS', *Eur Neuropsychopharmacol*, **23**(8), pp. 956-959.
- 38 Li, H., Zhu, X. & Fan, Y. (2018) 'Identification of multi-scale hierarchical brain functional networks using  
39 deep matrix factorization', *International Conference on Medical Image Computing and Computer-  
40 Assisted Intervention*, Springer.

- 1 Li, R., Ma, X., Wang, G., Yang, J. & Wang, C. (2016) 'Why sex differences in schizophrenia?', *Journal*  
2 *of translational neuroscience*, **1**(1), pp. 37-42.
- 3 Ma, S., Correa, N. M., Li, X. L., Eichele, T., Calhoun, V. D. & Adali, T. (2011) 'Automatic identification  
4 of functional clusters in fMRI data using spatial dependence', *IEEE Trans Biomed Eng*, **58**(12), pp. 3406-  
5 3417.
- 6 McGrath, J., Saha, S., Welham, J., El Saadi, O., MacCauley, C. & Chant, D. (2004) 'A systematic review  
7 of the incidence of schizophrenia: the distribution of rates and the influence of sex, urbanicity, migrant  
8 status and methodology', *BMC Med*, **2**, p. 13.
- 9 Miller, R. L., Pearlson, G. & Calhoun, V. D. (2019) 'Whole brain polarity regime dynamics are  
10 significantly disrupted in schizophrenia and correlate strongly with network connectivity measures', *PLoS*  
11 *One*, **14**(12), p. e0224744.
- 12 Miller, R. L., Yaesoubi, M., Turner, J. A., Mathalon, D., Preda, A., Pearlson, G., Adali, T. & Calhoun, V.  
13 D. (2016) 'Higher Dimensional Meta-State Analysis Reveals Reduced Resting fMRI Connectivity  
14 Dynamism in Schizophrenia Patients', *PLoS One*, **11**(3), p. e0149849.
- 15 Navarro, F., van Os, J., Jones, P. & Murray, R. (1996) 'Explaining sex differences in course and outcome  
16 in the functional psychoses', *Schizophr Res*, **21**(3), pp. 161-170.
- 17 Nawka, A., Kalisova, L., Raboch, J., Giacco, D., Cihal, L., Onchev, G., Karastergiou, A., Solomon, Z.,  
18 Fiorillo, A., Del Vecchio, V., Dembinskas, A., Kiejna, A., Nawka, P., Torres-Gonzales, F., Priebe, S.,  
19 Kjellin, L. & Kallert, T. W. (2013) 'Gender differences in coerced patients with schizophrenia', *BMC*  
20 *Psychiatry*, **13**, p. 257.
- 21 Saha, S., Chant, D., Welham, J. & McGrath, J. (2005) 'A systematic review of the prevalence of  
22 schizophrenia', *PLoS Med*, **2**(5), p. e141.
- 23 Seeman, M. V. (2019) 'Does Gender Influence Outcome in Schizophrenia?', *Psychiatric Quarterly*, **90**(1),  
24 pp. 173-184.
- 25 Shenton, M. E., Kikinis, R., Jolesz, F. A., Pollak, S. D., LeMay, M., Wible, C. G., Hokama, H., Martin,  
26 J., Metcalf, D., Coleman, M. & et al. (1992) 'Abnormalities of the left temporal lobe and thought disorder  
27 in schizophrenia. A quantitative magnetic resonance imaging study', *N Engl J Med*, **327**(9), pp. 604-612.
- 28 Shinn, A. K., Baker, J. T., Lewandowski, K. E., Öngür, D. & Cohen, B. M. (2015) 'Aberrant cerebellar  
29 connectivity in motor and association networks in schizophrenia', *Front Hum Neurosci*, **9**, p. 134.
- 30 Stephan, K. E., Baldeweg, T. & Friston, K. J. (2006) 'Synaptic plasticity and dysconnection in  
31 schizophrenia', *Biol Psychiatry*, **59**(10), pp. 929-939.
- 32 Woodruff, P. W., Wright, I. C., Bullmore, E. T., Brammer, M., Howard, R. J., Williams, S. C., Shapleske,  
33 J., Rossell, S., David, A. S., McGuire, P. K. & Murray, R. M. (1997) 'Auditory hallucinations and the  
34 temporal cortical response to speech in schizophrenia: a functional magnetic resonance imaging study',  
35 *Am J Psychiatry*, **154**(12), pp. 1676-1682.
- 36 Yaesoubi, M., Silva, R. F., Iraj, A. & Calhoun, V. D. (2020) 'Frequency-Aware Summarization of  
37 Resting-State fMRI Data', *Front Syst Neurosci*, **14**(16).
- 38